

# The Effect of Indocyanine Green Antimicrobial Photothermal/Photodynamic Therapy on the Expression of BCL-2 and BAX Messenger RNA Levels in Human Gingival Fibroblast Cells

Maryam Pourhajibagher<sup>1</sup>, Samira Gharesi<sup>2</sup>, Nasim Chiniforush<sup>3</sup>, Abbas Bahador<sup>4</sup>

<sup>1</sup> Dental Research Center, Dentistry Research Institute, Tehran University of Medical Sciences, Tehran, Iran

<sup>2</sup> Department of Genetics, Islamic Azad University, Tehran Medical Branch, Tehran, Iran

<sup>3</sup> Laser Research Center, Dentistry Research Institute, Tehran University of Medical Sciences, Tehran, Iran

<sup>4</sup> Oral Microbiology Laboratory, Department of Medical Microbiology, School of Medicine, Tehran University of Medical Sciences, Tehran, Iran

**Corresponding author:** Abbas Bahador, Oral Microbiology Laboratory, Department of Medical Microbiology, School of Medicine, Tehran University of Medical Sciences, Tehran, Iran; E-mail: abahador@sina.tums.ac.ir

**Received:** 5 Nov 2019 ♦ **Accepted:** 29 Dec 2019 ♦ **Published:** 30 June 2020

**Citation:** Pourhajibagher M, Gharesi S, Chiniforush N, Bahador A. The effect of indocyanine green antimicrobial photothermal/photodynamic therapy on the expression of BCL-2 and BAX messenger RNA levels in human gingival fibroblast cells. *Folia Med (Plovdiv)* 2020;62(2):314-23. doi: 10.3897/folmed.62.e48038.

## Abstract

**Background:** Antimicrobial photothermal/photodynamic therapy (PTT/PDT) with indocyanine green (ICG) is an adjuvant therapeutic approach in the treatment of periodontitis. To explore whether PTT/PDT with ICG causes cell death by apoptosis in human gingival fibroblast (HGF) cells, BAX and BCL-2 genes expression as key events for apoptosis were evaluated in this study.

**Materials and methods:** HGF cells were treated with: 1) different concentrations (500–2000 µg/mL) of ICG alone, 2) Diode laser irradiation alone with a fluency of 39.06 J/cm<sup>2</sup>; 3) PTT/PDT combined different concentrations (500–2000 µg/mL) of ICG with an 808 nm diode laser with a fluency of 39.06 J/cm<sup>2</sup>, and 4) controls (untreated cells). After that, BAX and BCL-2 messenger RNA levels were evaluated by real-time quantitative reverse transcription PCR.

**Results:** PTT/PDT with 500 µg/mL of ICG caused significant increases in the expression of the BAX gene, with an 8.5-fold increase, which was approximately 7- and 8.5-fold higher than PTT/PDT with ICG for 1500 and 2000 µg/mL of ICG, respectively, indicating induction of apoptosis in HGF cells. ICG (in different test concentrations), diode laser, and PTT/PDT with ICG (1500 and 2000 µg/mL of ICG) treatment displayed insignificant increases in expression levels of BAX (all  $p > 0.05$ ). Our experiments showed an insignificant increase (1.1–1.6-fold) in the expression of BCL-2 after ICG, diode laser, and PTT/PDT with ICG treatment (all  $p > 0.05$ ).

**Conclusions:** This study suggests that various concentration of ICG can be the diverse expression of BAX responses to PTT/PDT on HGF cells.

## Keywords

antimicrobial photothermal/photodynamic therapy, apoptosis, human gingival fibroblast cells, gene expression, indocyanine green, periodontitis, qRT-PCR

## BACKGROUND

Periodontitis is a multi-factorial inflammatory illness of the tooth-supporting structures and is associated with subgin-

gival bacterial biofilm formation; it is one of the major reasons of tooth loss.<sup>1</sup> Recently, the pathogenesis of periodontitis diseases has been explained by the alteration of normal apoptosis regulation. Apoptosis is a constitutive regulated

physiological process essential for the maintenance of cellular homeostasis in multicellular organisms that can be induced or inhibited by different stimuli.<sup>2-4</sup> It is also clear that *Aggregatibacter actinomycetemcomitans* and *Porphyromonas gingivalis* as periopathogen bacteria can induce significant apoptosis in monocytes and primary human gingival epithelial cells, respectively.<sup>5,6</sup> Microbial by-products including hydrogen sulfide and proteases can induce apoptosis in gingival epithelial cells and human gingival fibroblasts in the oral cavity, which may cause periodontal diseases.<sup>7,8</sup>

There are different treatment strategies for periodontitis, including surgical and non-surgical treatment. Antimicrobial photothermal/photodynamic therapy (PTT/PDT) is an adjuvant non-surgical approach used in the treatment of periodontal diseases.<sup>9,10</sup> In most studies, antimicrobial PTT/PDT is a beneficial adjunct for scaling and root planing (SRP), especially in chronic periodontitis treatment due to its ability to eliminate bacterial biofilms.<sup>11-13</sup> Combining antimicrobial PTT/PDT and SRP is beneficial, especially in lesions with untoward anatomic conditions.<sup>14</sup> Antimicrobial PTT/PDT as monotherapy shows advantages in cytokine modulation and is used as a non-invasive therapeutic method for the treatment of residual pockets and periodontal disease.<sup>15</sup> In antimicrobial PDT (aPDT), electron transfer in excited photosensitizers (PSs) can be done in two ways: Type I photoreaction which produces radicals and/or radical ions from substrates including highly reactive hydroxyl radicals (HO•) and Type II photoreaction which produces singlet oxygen (<sup>1</sup>O<sub>2</sub>).<sup>16,17</sup>

The efficiency of antimicrobial PTT/PDT is multifactorial and varies by the concentration and type of PS, and irradiation time and energy dose of the light. Different factors make PS ideal for aPDT, including high interaction with microbial cells and the optical window for sufficient tissue penetration of light.<sup>18</sup> More tissue penetration of 810 nm wavelength, as a near-infrared (NIR) diode laser system, then 635 nm and 660 nm, as the most common wavelength used in aPDT, has been addressed in recent studies.<sup>18,19</sup> Among the PSs that are active in this spectrum (i.e., 808 nm) can be referred to as indocyanine green (ICG). ICG is a member of the amphiphilic-tricarbocyanine dye family with the absorption peak around 808±5 nm, which is thought to be an effective PS against Gram-negative and Gram-positive bacteria. Although photo-activated ICG is known to yield <sup>1</sup>O<sub>2</sub>, it has been shown that photothermal (PTT) destruction of microbial cells was the dominant reaction.<sup>20,21</sup> ICG has also received Food and Drug Administration (FDA) approval to be used in clinical settings.<sup>19</sup>

The success of ICG antimicrobial PTT/PDT as a periodontal disease treatment not only is dependent on the effective decontamination of microorganisms but also via avoiding an unacceptable degree of harm to healthy periodontal tissue due to induction of apoptosis.<sup>22</sup> BAX (Bcl-2-associated X protein) and BCL-2 (B-cell lymphoma 2) are two members of the BCL-2 family that play an important role in apoptotic cell death. BAX (pro-apoptotic)

has been shown to promote cytochrome c release, which in turn leads to activation of caspases and degradation of specific protein substrates, whereas BCL-2 as an antiapoptotic protein blocks BAX-induced cytochrome c release and caspase activation, which can result in induction and inhibition of apoptotic cell death, respectively.<sup>22</sup> Thus, it has been suggested that the relative amounts of BAX and BCL-2 regulate the outcome of a living cell.<sup>23</sup> Because apoptosis has an extensive role in periodontal diseases, knowledge about the apoptosis response to ICG antimicrobial PTT/PDT in human gingival fibroblast (HGF) cells is necessary for its therapeutic intervention at different checkpoints. In this study, we determined the apoptosis response to PTT/PDT with ICG in HGF cells *in vitro* via evaluation of the expression of the apoptosis-related genes BAX and BCL-2 in HGF cells exposed to PTT/PDT with ICG. In this study, we hypothesize that there is a considerably significant difference between the expression of BAX and BCL-2 in HGF cells exposed to photo-activated ICG in different concentration. Under the null hypothesis, this difference is insignificant.

## MATERIALS AND METHODS

### Photosensitizer

A stock solution from ICG (Serva, Heidelberg), at concentrations of 4000 µg/mL was made by dissolving the ICG powder in a sterile balanced salt solution (BSS) at pH 7.4. The ICG solution was sterilized using a 0.22 µm syringe filter, and stored at 4°C in the dark before use.<sup>24</sup>

### Light source

An 808 nm diode laser (Konftec, DX82, Taiwan) with power output 250 mW was employed in this study. The output power density of the diode laser was determined by a power meter (Laser Point s.r.l., Milan, Italy).

### Cell culture

Human gingival fibroblast (HGF; IBRC C10459) cells were purchased from the Iranian Biological Resource Center (Tehran, Iran). The cells were grown in nutrient medium composed of Dulbecco's Modified Eagle's Medium (DMEM; Gibco, USA) supplemented with 10% fetal bovine serum (FBS; Sigma, USA), 1% penicillin-streptomycin solution (10,000 Unit/mL penicillin and 10 mg/mL streptomycin), 2 mM L-glutamine and 100 µg/mL of amphotericin B. Cells were incubated at 37°C in a humidified atmosphere of air (95%) and 5% CO<sub>2</sub>. Every 3 days the medium was changed. When the cultures reached 80% confluence, the cells were detached from the flasks by using 0.25% trypsin-0.02% ethylene diamine tetraacetic acid (EDTA) solution. For experiments requiring seeding of HGF cells in microplates,

in the third passages, a density of  $2 \times 10^6$  HGF cells/well were seeded in flat-bottom 96-well cell culture microplates (Greiner Bio-One, Germany).<sup>25</sup>

## Design of study

To determine the apoptosis response to an 808 nm diode laser, ICG and PTT/PDT with ICG in HGF cells *in vitro* via evaluation of apoptosis-related genes BAX and BCL-2 expression in treated HGF cells, test groups consisted of HGF cells subjected to:

- 1) ICG alone (in three concentrations 2000, 1500, and 500  $\mu\text{g}/\text{mL}$ ; L- P+; L and P stand for “light” and “photosensitizer,” respectively),
- 2) Diode laser alone with fluency of  $39.06 \text{ J}/\text{cm}^2$ , (L+ P-)
- 3) PTT/PDT with ICG; combined ICG (in three concentrations 2000, 1500, and 500  $\mu\text{g}/\text{mL}$ ) with 808 nm diode laser treatment with a fluency of  $39.06 \text{ J}/\text{cm}^2$  (L+ P+)
- 4) Control group (no exposure to either diode laser irradiation or ICG; L- P-)

## PTT/PDT procedure

The HGF cells (100  $\mu\text{L}$ ; at a final density of  $2 \times 10^6$  cells per well) were placed in each well of a sterile flat-bottom 96-well cell culture microplate. After HGF cells were grown until full confluence, the ICG (100  $\mu\text{L}$ ) was added for groups L- P+ and L+ P+, whereas sterile DMEM (100  $\mu\text{L}$ ) was added for groups L- P- and L+ P-. In the pre-irradiation time phase, the microplates were incubated for 5 min in a cell culture incubator. The microplate wells contents of groups L+ P+ and L+ P- were exposed to 808 nm the diode laser for 60 s ( $39.06 \text{ J}/\text{cm}^2$ ) in continuous mode at room temperature ( $25 \pm 2^\circ\text{C}$ ). The tip diameter was 7 mm and used in non-initiated mode. The probe of the laser was fixed 1 mm above the top surface of microplate by a microphone stand the total energy was 15 J. The microplate wells around the test wells of the microplates were filled with Indian ink to inhibit light emission to neighboring wells.<sup>14,15</sup> To avoid beam reflection from the tabletop during PTT/PDT with ICG, a sheet of black paper were used under the plates. The microplate wells in the control group did not receive any treatment. Next, cells in the microplate wells were scraped with a sterile tip of a pipette and transferred into 1.5-mL Eppendorf tubes, and three volumes of RNAlater® (Thermo Fisher Scientific, US) were then added to stabilize the RNA of HGF cells. The RNA of HGF cell suspensions were then extracted immediately.<sup>25</sup>

## RNA extraction

Collected HGF cells were centrifuged (13000  $\text{g} \times 10 \text{ min}$ ) and the pellet was washed twice with phosphate-buffered saline (PBS) (500  $\mu\text{L}$ ; pH 7.4). After the final centrifugation, the pellet of HGF cells was subjected to RNA extraction. For this purpose, the Hybrid-R™ Total RNA Purification Kit (GeneAll Biotechnology, Seoul, Korea) was used following the manufacturer’s recommended protocol.

## Assays for RNA integrity

Agarose gel electrophoresis was used to assess the integrity of the total extracted RNA. An aliquot of the RNA sample was run on a denaturing agarose gel stained with ethidium bromide (EB). The 18S and 28S ribosomal RNA (rRNA) bands were visualized by EB staining.

## Quantitation and evaluation of purity of extracted RNA

Ultraviolet (UV) spectroscopy using the NanoDrop® spectrophotometer (Thermo Fisher Scientific, US) at 260 nm and by measuring absorbance ratios at 260 vs 280 nm was used for quantification and evaluation of the purity of extracted RNA, respectively. Alternatively, to determine the purity of extracted RNA, we performed PCR using DNaseI treated RNA as a template. PCR amplification was performed in a final volume of 25  $\mu\text{L}$  containing 2  $\mu\text{L}$  of templates, 9  $\mu\text{L}$  of PCR master mix (Amplicon, Denmark), and 2.5 pM of each GAPDH forward and reverse primers. PCR was carried out in a thermal cycler apparatus (PeqStar; PeqLab, Germany) with an initial denaturation step (5 min at  $95^\circ\text{C}$ ), followed by 35 cycles including denaturation (1 min at  $95^\circ\text{C}$ ), annealing (30 s at  $59^\circ\text{C}$ ), and extension (30 s at  $72^\circ\text{C}$ ), with a final extension step (5 min at  $72^\circ\text{C}$ ). The results were analyzed by 2% agarose gel electrophoresis and subsequent staining with EB. HGF cells extracted DNA was used as a positive control in PCR amplification. Electrophoresis of extracted RNA on a denaturing gel showed intact RNA with sharp, clear 28S- and 18S rRNA bands (Fig. 1). As shown in Figure 1, the 28S rRNA band was approximately twice as intense as the 18S rRNA band. The 2:1 ratio of band intensity of 28S rRNA: 18S rRNA is an accepted indication of RNA Integrity. The results of this study showed that the RNA extracted from HGF cells ranged from 314.5

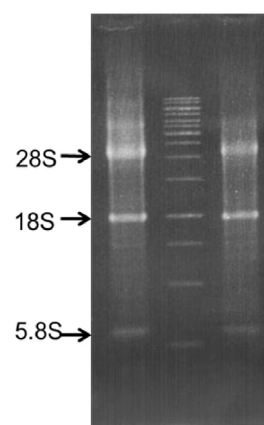


**Figure 1.** A 2% agarose gel electrophoresis of total RNA extraction from HGF cells. Lanes 1 and 3 represent samples collected before and after PTT/PDT with ICG, respectively. Lane 2 represents the DNA marker 1 kb. Five microliters of RNA were loaded for each sample.

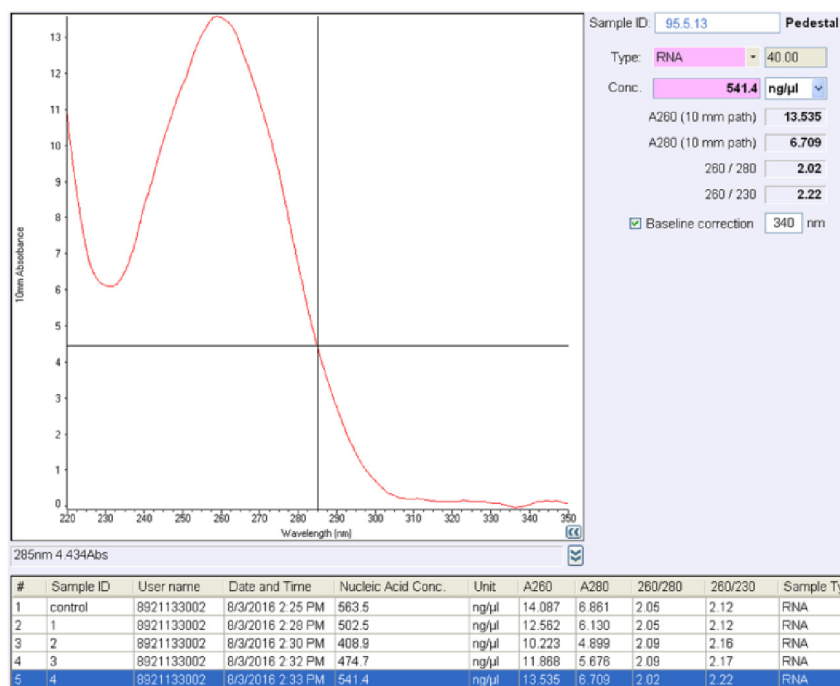


**Figure 2.** The concentration and purity of the total RNA. The 2.2 A260/A280 ratio indicates a high mRNA quality purified from total RNA.

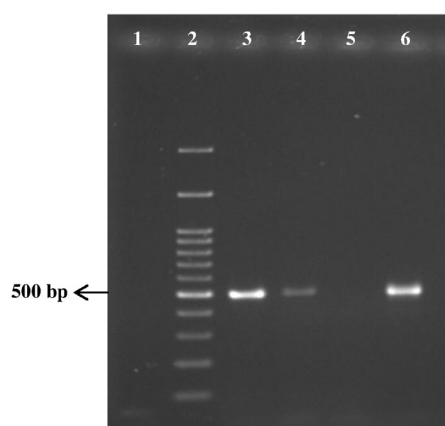


**Figure 3.** A 2% agarose gel electrophoresis of non-DNaseI treated RNA, DNase treated RNA, and cDNA after PCR. GAPDH was used as a housekeeping gene marker. Lanes 1, 2, 3, 4, 5, and 6 represent negative control, 100 bp marker, positive control, non treated RNA, treated RNA, and cDNA, respectively.

ng/ $\mu$ L to 560 ng/ $\mu$ L with a mean yield of 412.5 ng/mL (**Fig. 2**). On purity assessment of RNA extraction, we found that all samples were within the optimal range of  $\sim$ 2.0. The amplification of GAPDH by PCR yielded no bands in DNase I treated extracted RNA, indicating the purity of the DNaseI treated extracted RNA (**Fig. 3**).

### cDNA synthesis

One  $\mu$ g/ $\mu$ L of total extracted RNA was reverse transcribed into a cDNA template using a RevertAid First Strand cDNA

Synthesis Kit (Thermo Fisher Scientific, US). The quality and quantity of cDNA were estimated using ethidium bromide agarose gel electrophoresis and spectrophotometry, respectively. PCR was used to confirm cDNA synthesis from DNaseI-treated RNA as described in Section 2.3.2. As shown in **Fig. 3**, the amplification of GAPDH by PCR yielded a band in cDNA as the template, indicating the successful reverse transcription of total extracted RNA into a cDNA.

### Primers

All primers used in this study i.e., GAPDH forward primer, 5'-CGC TCT CTG CTC CTC CTG TT-3' and GAPDH reverse primer, 5'-ACG ACC AAA TCC GTT GAC TCC-3'; BAX forward primer, 5'-TTC TGA CGG CAA CTT CAA CTG G-3' and BAX reverse primer, 5'-AGG AAG TCC AAT GTC CAG CC-3'; and BCL-2 forward primer, 5'-AGG CTG GGA TGC CTT TGT GG-3' and BCL-2 reverse primer, 5'-GGG CAG GCA TGT TGA CTT CAC-3' were optimized to an equal melting temperature of 59°C. BAX primers were used from a previous study<sup>22</sup> and GAPDH, as well as BCL-2 primers, were designed via gene runner software version 3.05 (Hastings Software Inc. Hastings, NY, USA). To ensure the specificity of GAPDH and BCL-2 primers, their sequences were searched against GenBank sequences with the BLAST program.

### Determination of specificity of primers

To determine the specificity of the primers, the generation of a single amplicon of the correct size from each prim-

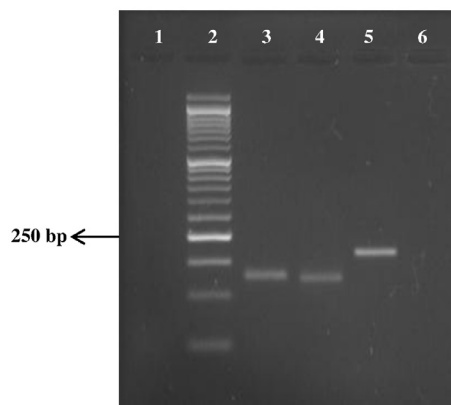


**Figure 4.** A 2% agarose gel electrophoresis of the specificity of the designed primers for detection of BAX, BCL-2, and GAPDH genes; Lanes 1, 2, 3, 4, and 5 represent negative control, DNA marker 50 bp, BAX amplicon, GAPDH amplicon, and BCL-2 amplicon, respectively.

er was evaluated on agarose gel electrophoresis. For this assessment, cDNA was subjected to PCR amplification as mentioned above (Section 2.3.2). Alternatively, Real-Time PCR methodologies utilizing SYBR Green dye (qRT-PCR Master Mix; Takara, Japan) was used to analyze melt curves to confirm the specificity of the amplified product. For this purpose, a default melting program was run on a real-time PCR machine (Bioer Technology, Hangzhou, China) at the end of the cycling program. The amplification of GAPDH, BAX, and BCL-2 by PCR yielded no false-positive bands in negative controls and unspecific bands in test samples (Fig. 4). The agarose gels of the amplified product revealed single bands corresponding to the predicted amplicon length. As shown in Fig. 5, dissociation melting curves of GAPDH, BAX, and BCL-2 amplicons with a single peak demonstrates the specificity of the primer pairs.

### Quantitative Real-time PCR

For the real-time reaction, a master mix was prepared as follows: 7  $\mu$ L water, 10  $\mu$ L SYBR green PCR Master Mix, 1

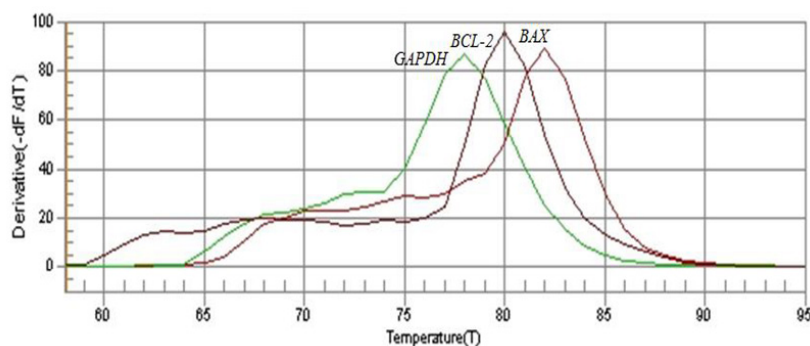


**Figure 5.** Melting curves of GAPDH, BAX, and BCL-2 amplicon. Dissociation curves with a single peak reveal the specificity of the primer pairs.

$\mu$ L cDNA as a PCR template, and 2  $\mu$ L volume of primers. A two-step experimental run protocol was used: 1) initial denaturation program (5 min at 95°C) and 2) 35 cycles of 15 s at 95°C, 15 s at 59°C, and 15 s at 72°C. Each PCR reaction was completed in triplicate. In this study, GAPDH used as a housekeeping gene for normalizing of test RNA expression.

### Statistical analysis

The data are presented as mean  $\pm$  standard deviation (SD) from three experiments. Fold differences in RNA expression were determined by the  $2^{-\Delta\Delta C_t}$  method.<sup>23</sup> Changes in RNA expression greater than or equal to twofold were considered significant.<sup>23</sup>

## RESULTS

To examine whether the expression of BAX and BCL-2 genes changed after diode laser (L+ P-), ICG (L- P+), or PTT/PDT with ICG (L+ P+) treatment, we compared the relative gene-specific messenger RNA quantities of HGF cells under-treated versus control (untreated; L- P-). The relative change in transcript expression levels of the BAX and BCL-2 genes among the treated HGF cells are shown as mean  $\pm$  SD relative change over basal levels (Fig. 6).

Among treated HGF cells, PTT/PDT with ICG in 500  $\mu$ g/mL of ICG with a fluency of 39.06 J/cm<sup>2</sup> revealed a significant increase in the expression of the BAX gene, with a 8.5-fold rise, which was approximately 7- and 8.5-fold higher than PTT/PDT with ICG in 1500 and 2000  $\mu$ g/mL of ICG with a fluency of 39.06 J/cm<sup>2</sup>, respectively (Fig. 6). According to Fig. 6, PTT/PDT with ICG treatment using 1500 and 2000  $\mu$ g/mL at fluency of 39.06 J/cm<sup>2</sup> displayed an insignificant increase in expression levels of the BAX and BCL-2 genes compared with untreated HGF cells (control group; all  $p > 0.05$ ). As Figure 6 reveals, our PTT/

PDT with ICG experiments showed that an insignificant increase (1.1-fold) in the expression of the BCL-2 gene was observed after exposure to ICG (500 µg/mL) plus diode laser at fluency of 39.06 J/cm<sup>2</sup> ( $p>0.05$ ) compared with the control group.

As shown in Fig. 6, the expression of the BAX and BCL-2 genes were upregulated 1.4- and 1.3-fold, respectively, following diode laser irradiation alone with a fluency of 39.06 J/cm<sup>2</sup> compared with the control group (both  $p>0.05$ ). There was no remarkable difference in expression of the BAX and BCL-2 genes following ICG treatment at concen-

tration of the effect of the ICG concentration in PTT/PDT on HGF cells and the BCL-2/BAX signaling pathway, the present study analyzed the effect of PTT/PDT on HGF cells based on different concentration of ICG.

ICG as a new PS is used in several therapeutic fields such as ocular tumor therapy, management of retinal disease, as well as treatment of local infections and inflammatory disease, owing to its outstanding achievements and clinically brilliant properties that are sufficiently suitable for treatment.<sup>39,40</sup> However, ICG has a low cytotoxicity, some studies have shown its toxic effects when used locally.<sup>41</sup> Ho et al.<sup>42</sup> exposed ARPE-19 (human retinal pigment epitheli-

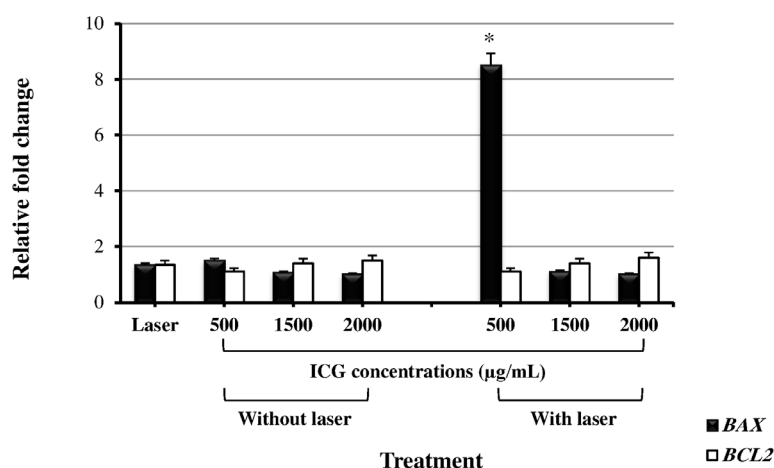


**Figure 6.** Effect of diode laser irradiation, ICG and PTT/PDT with ICG (at different concentrations) on the BAX and BCL-2 gene expression by HGF cells. qRT-PCR data for each gene were normalized against those obtained for the GAPDH control. The mRNA concentration was calculated as  $2^{-\Delta\Delta Ct}$  for each gene, where  $\Delta Ct$  represents the threshold cycle (CT) value of the gene subtracted from the CT value of the GAPDH control. Values are mean  $\pm$  standard error of the mean of cDNA concentrations for each gene transcript from three replicate experiments. \*,  $p<0.05$  significantly different from the control (HGF cells grown without treatment).

trations of 500–2000 µg/mL (all relative fold change < 2; all  $p>0.05$ ).

## DISCUSSION

The PTT/PDT is an adjuvant treatment approach and has gained approval for the treatment of various diseases such as local malignant and nonmalignant infectious diseases.<sup>26,27</sup> Numerous previous studies have also indicated the potential ICG antimicrobial role of PTT/PDT;<sup>28–33</sup> studies in *Staphylococcus aureus*, *Acinetobacter baumannii*, *A. actinomycetemcomitans*, and *P. gingivalis* demonstrated that aPDT reduced microbial pathogenicity,<sup>34–36</sup> suggesting that aPDT is an adjuvant treatment approach in microbial-associated diseases such as periodontitis. Several factors including the concentration of PS are involved in the success of aPDT.<sup>37</sup> PS concentration also plays an important role in cell cytotoxicity.<sup>38</sup> To further investigate the potential asso-

um) cells to 0.01 mg/mL of ICG for 3 h, 1 mg/mL of ICG for 20 min, and 5 mg/mL of ICG for 10 min without cytotoxicity. As in the Ho et al.<sup>42</sup> study, Peters et al.<sup>43</sup> stated that ICG did not exhibit cytotoxicity for ARPE-19 cells with an ICG concentration at or below 1250 µg/mL; however, with higher ICG concentrations, a toxic effect was observed. On the contrary to their study, Pourhajibagher et al.<sup>44</sup> research showed that PTT/PDT with ICG with a concentration of ICG at or below 750 µg/mL had cytotoxicity for HGF cells. This difference in results maybe because of the different cell types. Our PTT/PDT with ICG results on the effects of the concentration of ICG and irradiation time on the BCL-2/BAX signaling pathway is consistent with previous reports, which showed increasing irradiation time and decreasing the concentration of ICG during PTT/PDT was associated with decreases in cell viability due to reduced activity of mitochondrial dehydrogenase enzyme in HGF, rat embryonic precursor neurosensory retinal (R28), and ARPE-19 cells.<sup>43,45</sup>

The power output of the current irradiation setting was conducted with the average laser power density of 250 mW and the duration of exposure of 39.06 J/cm<sup>2</sup>, which were much lower than those which had a cytotoxic effect as a result of detectable temperature increase in cells or tissues within 60 s after administration.

In agreement with the study of Pourhajibagher et al.<sup>44</sup> the current study demonstrated that PTT/PDT with ICG in 500 µg/mL of ICG increased expression of the proapoptotic gene, BAX, in HGF cells. In this case, in line with the other studies,<sup>46-49</sup> it suggests cytochrome c-dependent apoptosis of the HGF cell line occurred through downregulation of the BCL2/BAX ratio, which may be stimulating mitochondrial depolarization and resulting in apoptosis. Previous studies support our findings that a reduction in BCL-2 levels inhibits cell proliferation and promotes apoptosis.<sup>50</sup> It has revealed that BCL-2 is predominantly localized in the mitochondria. The major biological function of homodimers of BAX is to promote apoptosis, while homodimers of BCL-2 inhibit apoptosis. When a BAX/BCL-2 heterodimer is formed, the anti-apoptotic function of BCL-2 is inhibited by BAX, resulting in the promotion of apoptosis.<sup>51</sup>

It has been observed that mRNA synthesis and translational control are important in the induction of p53 protein levels in response to apoptotic cues. p53 mRNA contains the internal ribosome entry site (IRES) element, which aids in protecting the mRNA from microRNAs induced silencing. IRES prepares for a selective translation of the specific mRNAs in periods of attenuation of cap-dependent translation by bypassing the requirement for the factors that are subject to inhibition during apoptosis. Therefore, mRNA translational regulation via the IRES is the main mechanism by which p53 can respond to the different apoptotic triggers the cell is exposed to.<sup>52</sup>

It has been revealed that singlet molecular oxygen (<sup>1</sup>O<sub>2</sub>) which produced under the photodynamic action of PSs is a potent inducer of apoptosis. Cleavage of caspase-3 and its target proteins such as lamin B and poly (ADP ribose) polymerase, a signature event of apoptosis, can be induced by the singlet oxygen.<sup>53</sup>

Along with the recent study that showed PTT/PDT with ICG has been demonstrated to be non-cytotoxic against HGF cells, in 1000–2000 µg/mL of ICG with fluency of 39.06 J/cm<sup>2</sup>,<sup>44</sup> the current study demonstrated that PTT/PDT with ICG does not significantly increase BAX gene expression in HGF cells at or above a 1500 µg/mL concentration of ICG with an irradiation time of 60 s. The data collected here demonstrated that PTT/PDT with ICG at high concentrations of ICG inhibited the BCL-2/BAX signaling pathway. These data are supported by a previous study that revealed PTT/PDT with ICG at 1000 µg/mL concentrations of ICG inhibited this signaling pathway.<sup>25</sup>

Pourhajibagher et al.<sup>44</sup> in their recent investigations observed a reduction in the viability of cells when exposed to a light source alone. Nowak et al.<sup>37</sup> found that light exposure

can produce thermal injury in RPE cells, whereas exposure to light for longer periods can lead to photochemical damage of treated cells. Contrary to the above studies, according to our results no significant increase in the expression of BAX and BCL-2 genes was observed in the treatment group with only a diode laser when compared to controls.

This is the first study that shows the phototoxicity mechanism of ICG during irradiation by a laser. It has been shown that the major mechanism after ICG excitation by diode laser is the transformation of 88% of energy to heat inside the ICG molecules for PTT. The residual energy can generate singlet oxygen for PDT. So, the mechanism of action is more PTT rather than photodynamic action.<sup>54,55</sup>

We hypothesize that photo-activated ICG can be hazardous to HGF cells due to its photothermal activity and on a smaller scale <sup>1</sup>O<sub>2</sub>-mediated DNA and membrane damage, which possibly leads to induction of apoptosis and ultimately cell death. Therefore, PTT/PDT with ICG as an adjuvant treatment should avoid using a low concentration of ICG (below 1000 µg/mL) and as much as possible, the intervention location should be kept dry, which can prevent dilution of ICG. In the present study, we found that ICG in lower concentrations had a photo-enhancing effect on the expression levels of BAX in HGF cells. High concentrations (1500 and 2000 µg/mL) of ICG, that did not elicit a thermal cytotoxic effect, also achieved insignificant increases in photo-enhancing effect in expression levels of BAX after irradiation. Although lower-temperature light-induced hyperthermia (<42°C) is identified to be synergistic with PDT<sup>56</sup>, the power intensity used in PDT treatment in this study was restricted explicitly in order to avoid significant tissue heating so that the photochemical reactions were dominant and the thermal effects did not alter the effective dose administered. Thus, the concentration of ICG should be a primary concern for the management of local infection and human health. Therefore, the optimum concentration of ICG for PTT/PDT should be at least 1000 µg/mL with a 60 s irradiation time. Further studies are needed to confirm our data and functional studies are necessary to establish a possible causal relationship between PTT/PDT with ICG and apoptosis.

## CONCLUSIONS

Our results demonstrated that the PTT/PDT with ICG at low concentration of ICG had a positive effect on BAX gene expression, resulting in induction of apoptosis in HGF cells induced by the PTT/PDT procedure. The concentration of ICG applied should be considered as a crucial point for PTT/PDT as an adjuvant therapeutic approach. It is recommended to use ICG not only the best ICG antimicrobial effect in PTT/PDT, but also less effect on the induction of apoptosis in human cells with a concentration at or above 1000 µg/mL.

## Acknowledgements

This research has been supported by Laser Research Center of Dentistry (LRCD), Dentistry Research Institute, Tehran University of Medical Sciences & Health Services grant No. 94-04-97-30540.

## Conflict of Interest

The authors declare that there is no conflict of interests regarding the publication of this paper.

## REFERENCES

1. Slots J. Periodontitis: facts, fallacies and the future. *Periodontol* 2017; 75:7–23.
2. Gamonal J, Bascones A, Acevedo A, et al. Apoptosis in chronic adult periodontitis analyzed by in situ DNA breaks, electron microscopy, and immunohistochemistry. *J Periodontol* 2001; 72:517–25.
3. Mori G, Brunetti G, Colucci S, et al. Alteration of activity and survival of osteoblasts obtained from human periodontitis patients: role of TRAIL. *J Biol Regul Homeost Agents* 2007; 21:105–14.
4. Di Benedetto A, Gigante I, Colucci S, et al. Periodontal disease: linking the primary inflammation to bone loss. *Clin Dev Immunol* 2013; 2013: 503754.
5. Kelk P, Johansson A, Claesson R, et al. Caspase 1 involvement in human monocyte lysis induced by *Actinobacillus actinomycetemcomitans* leukotoxin. *Infect Immun* 2003; 71:4448–55.
6. Stathopoulou PG, Galicia JC, Benakanakere MR, et al. *Porphyromonas gingivalis* induce apoptosis in human gingival epithelial cells through a gingipain-dependent mechanism. *BMC Microbiol* 2009; 27: 1–12.
7. Murata T, Yaegaki K, Qian W, et al. Hydrogen sulfide induces apoptosis in epithelial cells derived from human gingival. *J Breath Res* 2008; 2: 1–6.
8. Galicia JC, Benakanakere MR, Stathopoulou PG, et al. Neutrophils rescue gingival epithelial cells from bacterial-induced apoptosis. *J Leukoc Biol* 2009; 86: 181–6.
9. Chitsazi MT, Shirmohammadi A, Pourabbas R, et al. Clinical and microbiological effects of photodynamic therapy associated with non-surgical treatment in aggressive periodontitis. *J Dent Res Dent Clin Dent Prospects* 2014; 8: 153–9.
10. Balata ML, Andrade LP, Santos DB, et al. Photodynamic therapy associated with full-mouth ultrasonic debridement in the treatment of severe chronic periodontitis: a randomized-controlled clinical trial. *J Appl Oral Sci* 2013; 21: 208–14.
11. Ge LH, Shu R, Shen MH. Effect of photodynamic therapy on IL-1beta and MMP-8 in gingival crevicular fluid of chronic periodontitis. *Shanghai Kou Qiang Yi Xue* 2008; 17: 10–4.
12. Palmer A. Periodontitis among adults aged  $\geq 30$  years - United States, 2009-2010. *MMWR Suppl* 2013; 62: 129-35.
13. Harris DM, Yessik M. Therapeutic ratio quantifies laser antiseptics: Ablation of *Porphyromonas gingivalis* with dental lasers. *Lasers Surg Med* 2004; 35: 206–13.
14. Prasanth CS, Karunakaran SC, Paul AK. Antimicrobial photodynamic efficiency of novel cationic porphyrins towards periodontal Gram-positive and Gram-negative pathogenic bacteria. *Photochem Photobiol* 2014; 90: 628–40.
15. Kolbe MF, Ribeiro FV, Luchesi VH. Photodynamic therapy during supportive periodontal care: clinical, microbiologic, immunoinflammatory, and patient-centered performance in a split-mouth randomized clinical trial. *J Periodontol* 2014; 85: 277–86.
16. Baptista MS, Cadet J, Di Mascio P, et al. Type I and type II photosensitized oxidation reactions: guidelines and mechanistic pathways. *Photochem Photobiol* 2017; 93(4): 912–9.
17. Plaetzer K, Krammer B, Berlanda J, et al. Photophysics and photochemistry of photodynamic therapy: fundamental aspects. *Lasers Med Sci* 2009; 24(2): 259–68.
18. Sperandio FF, Huang YY, Hamblin MR. Antimicrobial photodynamic therapy to kill Gram-negative bacteria. *Recent Pat Antiinfect Drug Discov* 2013; 8: 108–20.
19. Chen J, Liu C, Zeng G, et al. Indocyanine green loaded reduced Graphene Oxide for in vivo photoacoustic/fluorescence dual-modality tumor imaging. *Nanoscale Res Lett* 2016; 11: 1–11.
20. Engel E, Schraml R, Maisch T, et al. Light-induced decomposition of indocyanine green. *Invest Ophthalmol Vis Sci* 2008; 49(5): 1777–83.
21. Boehm TK, Ciancio SG. Diode laser activated indocyanine green selectively kills bacteria. *J Int Acad Periodontol* 2011; 13(2): 58–63.
22. Reinhard A, Sandborn WJ, Melhem H, et al. Photodynamic therapy as a new treatment modality for inflammatory and infectious conditions. *Expert Rev Clin Immunol* 2015; 11: 637–57.
23. Yin XM, Oltvai ZN, Korsmeyer SJ. BH1 and BH2 domains of Bcl-2 are required for inhibition of apoptosis and heterodimerization with Bax. *Nature* 1994; 369: 321–3.
24. Sobeh MS, Chan P, Ham RJ, et al. Photodynamic therapy in a cell culture model of human intimal hyperplasia. *Eur J Vasc Endovasc Surg* 1995;9:463-468.
25. Ghareis S, Pourhajbagher M, Chiniforush N, et al. Effect of photodynamic therapy based on indocyanine green on expression of apoptosis-related genes in human gingival fibroblast cells. *Photodiagnosis Photodyn Ther* 2017; 19: 33–6.
26. Awan MA, Tarin SA. Review of photodynamic therapy. *Surgeon* 2006; 4: 231–6.
27. Huang Z. A review of progress in clinical photodynamic therapy. *Technol Cancer Res Treat* 2005; 4: 283–93.
28. Pourhajbagher M, Chiniforush N, Ghorbanzadeh R, et al. Photo-activated disinfection based on indocyanine green against cell viability and biofilm formation of *Porphyromonas gingivalis*. *Photodiagn Photodyn Ther* 2017; 17: 61–4.
29. Pourhajbagher M, Chiniforush N, Shahabi S, et al. Sublethal doses of photodynamic therapy affect biofilm formation ability and metabolic activity of *Enterococcus faecalis*. *Photodiagn Photodyn Ther* 2016; 15: 159–66.
30. Pourhajbagher M, Chiniforush N, Raoofian R, et al. Effects of sublethal doses of photo-activated disinfection against *Porphyromonas gingivalis* for pharmaceutical treatment of periodontal-endodontic lesions. *Photodiagn Photodyn Ther* 2016; 16: 50–3.
31. Pourhajbagher M, Ghorbanzadeh R, Parker S, et al. The evaluation of cultivable microbiota profile in patients with secondary endodontic infection before and after photo-activated disinfection. *Photodiagnosis Photodyn Ther* 2017; 18: 198–203.

32. Pourhajibagher M, Monzavi A, Chiniforush N, et al. Real-Time Quantitative Reverse Transcription-PCR analysis of expression stability of *Aggregatibacter actinomycetemcomitans* fimbria-associated gene in response to photodynamic therapy. *Photodiagn Photodyn Ther* 2017; 18: 78–82.
33. Beytollahi L, Pourhajibagher M, Chiniforush N, et al. The efficacy of photodynamic and photothermal therapy on biofilm formation of *Streptococcus mutans*: An in vitro study. *Photodiagnosis Photodyn Ther* 2017; 17: 55–60.
34. Pourhajibagher M, Chiniforush N, Shahabi S, et al. Monitoring gene expression of *rcpA* from *Aggregatibacter actinomycetemcomitans* versus antimicrobial photodynamic therapy by relative quantitative real-time PCR. *Photodiagnosis Photodyn Ther* 2017; 19: 51–5.
35. Pourhajibagher M, Boluki E, Chiniforush N, et al. Modulation of virulence in *Acinetobacter baumannii* cells surviving photodynamic treatment with toluidine blue. *Photodiagnosis Photodyn Ther* 2016; 15: 202–12.
36. Hoorijani MN, Rostami H, Pourhajibagher M, et al. The effect of antimicrobial photodynamic therapy on the expression of novel methicillin resistance markers determined using cDNA-AFLP approach in *Staphylococcus aureus*. *Photodiagnosis Photodyn Ther* 2017; 19: 249–55.
37. Wang Y, Zuo Z, Liao X, et al. Investigation of photodynamic therapy optimization for port wine stain using modulation of photosensitizer administration methods. *Exp Biol Med* 2013; 238: 1344–9.
38. Thomas CD, Poyer F, Maillard P, et al. Cellular density, a major factor involved in PDT cytotoxic responses: study on three different lines of human retinoblastoma grafted on nude mice. *Photodiagn Photodyn Ther* 2015; 12: 267–75.
39. Fineman MS, Maguire JJ, Fineman SW, et al. Safety of indocyanine green angiography during pregnancy: a survey of the retina, macula, and vitreous societies. *Arch Ophthalmol* 2001; 119: 353–5.
40. Mahmood K, Zia KM, Zuber M, et al. Recent developments in curcumin and curcumin based polymeric materials for biomedical applications: a review. *Int J Biol Macromol* 2015; 81: 877–90.
41. Grisanti S, Szurman P, Gelissen F, et al. Histological findings in experimental macular surgery with indocyanine green. *Invest Ophthalmol Vis Sci* 2004; 45: 282–6.
42. Ho JD, Tsai RJ, Chen SN, et al. Cytotoxicity of indocyanine green on retinal pigment epithelium: implications for macular hole surgery. *Arch Ophthalmol* 2003; 121: 1423–9.
43. Peters S, Altwater A, Bopp S, et al. Systematic evaluation of ICG and trypan blue related effects on ARPE-19 cells in vitro. *Exp Eye Res* 2007; 85: 880–9.
44. Pourhajibagher M, Chiniforush N, Parker S, et al. Evaluation of antimicrobial photodynamic therapy with indocyanine green and curcumin on human gingival fibroblast cells: An in vitro photocytotoxicity investigation. *Photodiagnosis Photodyn Ther* 2016; 15: 13–8.
45. Narayanan R, Kenney MC, Kamjoo S, et al. Toxicity of indocyanine green (ICG) in combination with light on retinal pigment epithelial cells and neurosensory retinal cells. *Curr Eye Res* 2005; 30: 471–8.
46. Ahmad N, Gupta S, Feyes DK, et al. Involvement of Fas (APO-1/CD95) during photodynamic therapy-mediated apoptosis in human epidermoid carcinoma A431 cells. *J Invest Dermatol* 2000; 115: 1041–6.
47. Ali SM, Chee SK, Yuen GY, et al. Photodynamic therapy induced Fas-mediated apoptosis in human carcinoma cells. *Int J Mol Med* 2002; 9: 257–70.
48. Olivo M, Ali-Seyed M. Apoptosis-signalling mechanisms in human cancer cells induced by Calphostin-PDT. *Int J Oncol* 2007; 30: 537–48.
49. Chen B, Roskams T, Xu Y, et al. Photodynamic therapy with hypericin induces vascular damage and apoptosis in the RIF-1 mouse tumor model. *Int J Cancer* 2002; 98: 284–90.
50. He GF, Bian ML, Zhao YW, et al. A study on the mechanism of 5-aminolevulinic acid photodynamic therapy in vitro and in vivo in cervical cancer. *Oncol Rep* 2009; 21: 861–8.
51. Liu L, Yu X, Guo X, et al. miR-143 is downregulated in cervical cancer and promotes apoptosis and inhibits tumor formation by targeting Bcl-2. *Mol Med Rep* 2012; 5: 753–60.
52. Liwak U, Faye MD, Holcik M. Translation control in apoptosis. *Exp Oncol* 2012; 34(3): 218–30.
53. Kim SY, Lee SM, Tak JK, et al. Regulation of singlet oxygen-induced apoptosis by cytosolic NADP<sup>+</sup> dependent isocitrate dehydrogenase. *Mol Cell Biochem* 2007; 302(1-2): 27–34.
54. Shirata C, Kaneko J, Inagaki Y, et al. Near-infrared photothermal/photodynamic therapy with indocyanine green induces apoptosis of hepatocellular carcinoma cells through oxidative stress. *Sci Rep* 2017, p. 13958, 10.1038/s41598-017-14401-0
55. Reindl A, Penzkofer SH, Gong M, et al. Quantum yield of triplet formation for indocyanine green. *Journal of Photochemistry and Photobiology A: Chemistry* 1997; 105: 65–8.
56. Wilson BC, Weersink RA. The Yin and Yang of PDT and PTT. *Photochem Photobiol*. 2019. doi: 10.1111/php.13184.

# Влияние антимикробной фототермической / фотодинамической терапии индоцианиновым зелёным на экспрессию уровней BCL-2 и BAX в матричной РНК в клетках фибробластов десны человека

Маиям Поурхаджибагхер<sup>1</sup>, Самира Гхареси<sup>2</sup>, Насим Чинифоруш<sup>3</sup>, Аббас Бахадор<sup>4</sup>

<sup>1</sup> Дентальный исследовательский центр, Дентальный исследовательский институт, Университет медицинских наук Тегеран, Иран

<sup>2</sup> Кафедра генетики, Исламский университет Азад, Медицинский факультет, Тегеран, Иран

<sup>3</sup> Лазерный исследовательский центр, Дентальный исследовательский институт, Университет медицинских наук Тегеран, Иран

<sup>4</sup> Лаборатория оральной микробиологии, Кафедра медицинской микробиологии, Медицинский факультет, Университет медицинских наук Тегеран, Иран

**Автор для корреспонденции:** Аббас Бахадор, Лаборатория оральной микробиологии, Кафедра медицинской микробиологии, Медицинский факультет, Университет медицинских наук Тегеран, Иран; E-mail: abahador@sina.tums.ac.ir

**Дата получения:** 5 ноября 2019 ♦ **Дата приемки:** 29 декабря 2019 ♦ **Дата публикации:** 30 июня 2020

**Образец цитирования:** Pourhajibagher M, Gharezi S, Chiniforush N, Bahador A. The effect of indocyanine green antimicrobial photothermal/photodynamic therapy on the expression of BCL-2 and BAX messenger RNA levels in human gingival fibroblast cells. *Folia Med (Plovdiv)* 2020;62(2):314-23. doi: 10.3897/folmed.62.e48038.

## Резюме

**Введение:** Антимикробная фототермическая / фотодинамическая терапия (ФТТ/ФДТ) с индоцианиновым зелёным (ИЦЗ) является адъювантным терапевтическим подходом в лечении периодонтита. Чтобы выяснить, вызывает ли ИЦЗ -индуцированная ФТТ/ФДТ гибель клеток в результате апоптоза в клетках фибробластов десны человека (КФДЧ), в этом исследовании оценивали экспрессию генов BCL-2 и BAX в качестве ключевых событий для апоптоза.

**Материалы и методы:** Клетки КФДЧ обрабатывали 1) различными концентрациями (500–2000 µg/mL) только ИЦЗ, 2) облучением диодным лазером с плотностью 39,06 J/cm<sup>2</sup>; 3) ФТТ/ФДТ, объединённые в различных концентрациях (500–2000 500–2000 µg/mL) ИЦЗ с диодным лазером 808 нм с плотностью 39,06 J/cm<sup>2</sup>, и 4) контроли (необработанные клетки). Затем уровни BCL-2 и BAX в мРНК измеряли количественной ПЦР с обратной транскриптазой в реальном времени.

**Результаты:** ФТТ/ФДТ с 500 µg/mL ИЦЗ привели к значительному увеличению экспрессии гена BAX в 8,5 раз, что было примерно в 7 и 8,5 раз выше, чем соответственно ФТТ/ФДТ с 1500 и 2000 µg/mL ИЦЗ, который является индикатором индукции апоптоза в клетках КФДЧ. Обработка ИЦЗ (в различных тестовых концентрациях), диодным лазером и ФТТ/ФДТ с ИЦЗ (1500 и 2000 µg/mL ИЦЗ) показала значительное увеличение уровней экспрессии I – V (все p > 0,05). Наш эксперимент показал значительное увеличение (в 1,1–1,6 раза) экспрессии BCL-2 после лечения с помощью ИЦЗ, диодного лазера и ФТТ/ФДТ с ИЦЗ (все p > 0,05).

**Выводы:** Это исследование показало, что различные концентрации ИЦЗ могут быть разнообразной экспрессией ответов BAX на ФТТ/ФДТ клеток КФДЧ.

## Ключевые слова

антимикробная фототермическая / фотодинамическая терапия, апоптоз, клетки фибробластов десны человека, экспрессия генов, индоцианиновый зелёный, периодонтит, qRT-PCR